Preliminary study for the suitability of eucalyptus chips and coal for combustion in a fluidized bed reactor

Angenor Geovani Auler[1] , Matheus Vilares Mem de Sá[1] , Paulo Eichler[1] , Jaqueline Lidorio de Mattia[1] , Guilherme Silva[1] , Guilherme de Souza[1] ,Fernando Almeida Santos[1]

[1]Universidade Estadual do Rio Grande do Sul, Rua Inconfidente, 395, Bairro Primavera, CEP 93340-140, Novo Hamburgo, RS, Brazil

Abstract - The combustion with fluidized bed reactors has as main advantages the best energy utilization of combustible materials and a lower generation of pollutants. The fluidization success depends on the characteristics of the particles that compose the bed. This research aimed to perform a preliminary evaluation and characterization of the energy potential and the fluidization curves in fluidized beds formed by binary mixtures of eucalyptus chips + sand and mineral coal + sand. We tested: 1) physical characterization of solid fuels; 2) chemical characterization of combustible materials; 3) thermogravimetric analysis of fuels; 4) determination of the fluidization curves and minimum fluidization velocity for a polydisperse bed. We observed 19.15 MJ kg^{-1} of lower calorific value for eucalyptus chips and 10.1 MJ kg^{-1} for coal. The increase in biomass percentage in mixture caused a pressure drop in bed, indicating the formation of preferred paths and a necessity to increase fluid velocity. The fluidization of coal and Eucalyptus chips can be viable in a bubbling fluid bed process, motivating future theoretical and experimental studies involving the application of this methodology in the development of clean and sustainable technologies.

Estudo preliminar para combustão de cavacos de eucalipto e carvão em um reator de leito fluidizado

Resumo - A combustão com reatores de leito fluidizado tem como principais vantagens o melhor aproveitamento energético de materiais combustíveis e uma menor geração de poluentes. O sucesso da fluidização depende das características das partículas que compõem o leito. O objetivo deste trabalho foi avaliar e caracterizar o potencial energético e as curvas de fluidização em leitos fluidizados formados por misturas binárias de cavacos de eucalipto + areia e carvão mineral + areia. Realizaram-se as seguintes análises e etapas: 1) caracterização física dos materiais; 2) caracterização química de materiais combustíveis; 3) análise termogravimétrica dos combustíveis; 4) determinação das curvas de fluidização e velocidade mínima de fluidização para um leito polidisperso. Foi obtido poder calorífico inferior de 19,15 MJ kg^{-1} para o cavaco de eucalipto e 10,1 MJ kg^{-1} para carvão. O aumento da porcentagem de biomassa na mistura causou queda de pressão no leito, indicando a formação de caminhos preferenciais e a necessidade de aumentar a velocidade do fluido. A fluidização de cavacos de eucalipto e carvão pode ser viável para aplicação em um processo de leito fluidizado borbulhante, motivando futuros estudos teóricos e experimentais envolvendo esta metodologia no desenvolvimento de tecnologias limpas e sustentáveis.

A. G. Auler1 et al.

Introduction

The fossil fuels, which are finite and highly polluting, are being replaced by renewable energy sources such as hydro, solar, wind, and biomass. Biomass has as advantageous characteristics the versatility and capacity to be stored in several ways, allowing the production of liquid, solid or gaseous fuels and electricity (Vaz Júnior et al., 2011; Santos et al., 2013). The United Nations Framework Convention on Climate Change (UNFCCC) defines biomass as non-fossilized and biodegradable organic material originating from plants, animals and microorganisms (UNFCCC, 2019). Eichler et al. (2015) define lignocellulosic biomass as a renewable raw material for energy production and with great processing potential for conversion into more elaborated bioenergetic forms for the final use, of every form of energy accumulated through photosynthetic processes. Because of its abundance, availability and renewable character, it is a promising source for bioenergy and bioproducts (Santos et al., 2013; Phitsuwan et al., 2013; Rambo et al., 2015; Linhares, 2016). The energy potential of biomass can be used in a biorefinery through the chemical, biochemical or thermochemical routes.

When the combustion occurs in fluidized bed reactors, conversion of biomass into bioelectricity is more efficient (Suksankraisorn et al., 2010). Fluid bed refers to a bed of finely divided solids through which a gas or liquid passes giving a similar appearance to a boiling liquid (Gomes, 2017). Due to the higher contact surface between the upward fluid in the bed and the fuel to be fluidized, it occurs the homogenization of temperature in the reactor, resulting in higher rates of heat and mass transfer (Bioetanol..., 2008, Santos et al., 2013; Phitsuwan et al., 2013, Rambo et al., 2015). To increase efficiency using this technology, Paudel & Feng (2013) showed the necessity to add an inert material with higher sphericity in the bed, such as sand, calcite, or alumina. Nevertheless, Linhares (2016) and Pereira (2017) mentioned the difficulty of fluidization caused by the formation of preferential paths in the bed or by the segregation of the mixture parts due to the presence of high biomass proportions. Therefore, it is necessary to establish the correct amount of biomass to coal and sand proportions to achieve correct fluidization characteristics in the bed.

According to the International Energy Agency (IEA), coal is the fossil fuel with the highest availability and

with reserves on all continents. The coal industry is well established, generating jobs and income. It is a low-cost fuel with intense participation in the world's energy generation and it is a strategic factor for the energy security, being the main fuel source used in thermoelectric power plants (IEA, 2016). Therefore, it is an interesting solid fuel to be utilized as energetic parameter in fluidized bed studies. Also, as coal is considered a fossil fuel and it is not interesting to be used alone for energetic purposes, it is highly desirable to use a renewable fuel with high calorific potential such as Eucalyptus wood.

The Eucalyptus is native to Oceania and Southeast Asia, composed of more than 700 species. Eucalyptus is one of the best options for the formation of energetic forests since it can be cultivated in several regions with different edaphoclimatic conditions (Santos, 2013; AGEFLOR, 2016). It occupies more than 72% of the Brazilian planted forest area (IBÁ, 2017). Eucalyptus plantations are present in more than 200 municipalities in Rio Grande do Sul State. The largest forests, inside the State, are located in the Central-South regions (AGEFLOR, 2017), in the surroundings of the main Brazilian mineral coal reserve, located in Candiota (Brasil, 2011). The President Médice Thermal Power Plant project, located in Candiota, can generate 446 MW and will have a capability to generate 796 MW after conclusion of phase 3. This Plant uses coal as a combustible to generate electricity (Brasil, 2019).

The objective of the present paper was to perform a preliminary evaluation and characterization of the energy potential and the fluidization curves in fluidized beds formed by binary mixtures of eucalyptus chips + sand and mineral coal + sand. The results can motivate future theoretical and experimental studies involving the application of this methodology in the development of cleaner and sustainable technologies.

Material and methods

The experiments were carried out at the Science and Technology Foundation (CIENTEC), at the Pontifical Catholic University of Rio Grande do Sul (PUCRS) and at the Federal University of Viçosa (UFV).

We used Eucalyptus chips and coal as fuels. The sand was used as an inert material because of its low cost and its ease acquisition.

The mineral coal, supplied by Companhia Rio-grandense de Mineração (CRM), came from the Candiota deposit located in the municipality of Candiota, RS, Brazil. The Eucalyptus chips, from *Eucalyptus* spp. was supplied by the CMPC – Celulose Riograndense, located in the municipality of Guaíba, RS, Brazil. The sand was acquired in the commercial center of Canoas, RS, Brazil.

Fuels' characterization

To characterize the fuels, we performed immediate analysis, elemental analysis, the use of a calorimetric pump to determine their gross calorific value and the thermogravimetric analyses.

In the immediate analysis, according to Abreu (2015), moisture, ash, volatile matter, and fixed carbon were analyzed.

Three 50 mL porcelain crucible were weighed, previously dried in an oven at 105 ºC for 4 h and placed in a desiccator until room temperature in order to determine the moisture content. Three samples of 1 g of material were weighed in the beakers. Afterward, these samples were taken to the oven at 105 ºC until reaching a constant mass with a variation of ± 0.001 g in the present moisture after 1 h of sample reheating. After this period, the samples were removed from the oven and placed in a desiccator at room temperature and weighed again, according to ABNT NBR 8293 (ABNT, 1983c).

The ash content determination was performed according to ABNT NBR 8290. The ashes obtained are the result of the complete oxidation of the combustible material, composed of inorganic constituents (ABNT, 1983a).

The determination of the volatile content was done according to ABNT NBR 8290. After determining the moisture content, the sample was placed in a Quimis Q318M muffle furnace at approximately 950 ºC for 7 min. The sample was then placed in a desiccator for cooling and subsequent weighing (ABNT, 1983b).

The determination of the fixed carbon content was made by the difference of the results of moisture, ash and volatile contents using Equation 1 (ABNT, 1983d).

$$Tcf = 100 - (Tu+Tc+Tv) \qquad (1)$$

Where: Tcf = fixed carbon content; Tu = moisture content; Tc = ash content; Tv = volatile content.

The elemental analysis was based on the Pregl-Dumas method, that is an automated calorimetric method (Patterson 1973). The samples were burned in the Leco brand non-dispersive TRUSPEC® elemental analyzer equipped with an infrared detector. In this equipment, the samples were burned in an oxygen atmosphere at 950 ºC.

Sulfur analysis, in total percentage, was performed on the Leco SC-632® elemental analyzer equipped with an infrared detector. In this equipment, the samples were burned under an oxygen atmosphere at 1,350 ºC.

The calorific value was obtained by placing a 350 mL sample of the combustible material inside a calorimetric pump. The calorimetric pump was equipped with an ignition device through an electric current. The lower calorific value (LCV) was determined by the Equation 2.

$$LCV = \frac{6318}{M} * 4.186 \qquad (2)$$

Where: M = the combustible sample's mass; 6318 = constant equivalent to the energy of 1 gof standard calibration substance of the calorimeter (benzoic acid); 4.186 is the conversion rate from cal g^{-1} to kJ kg^{-1}.

The analysis of the Eucalyptus chips and the coal samples thermal degradation´s characteristics were obtained through thermogravimetric analyzes (TGA) performed with a 20 mg sample in a thermobalance Perkin Elmer TGA7® under 20 mL min^{-1} airflow and 10 ºC min^{-1} heating rate, starting at 30 ºC.

Materials' physical properties

The determination of physical characteristics of combustible materials, such as particle size, apparent and real densities, and Sauter diameter, were carried out in the CIENTEC process laboratory.

The average diameter of Sauter was used for the determination of the mineral coal's and the sand's average particle size.

The granulometric determination of the Eucalyptus chips was performed using the equivalent diameter method. In order to determine the average diameter of the Eucalyptus chips, which are reminiscent of a parallelepiped, the sample was quartered and the two opposing sides were mixed. This procedure was repeated three times. After the final blocking, the Eucalyptus chips contained therein were individually measured (length, width, and diameter) with a digital caliper DIGIMESS®.

The volume was obtained by multiplying the three dimension values. The equivalent diameter was obtained by Equation 3 (Dioguardi & Mele, 2015).

$$D_{eq} = \sqrt[3]{V/\pi} \qquad (3)$$

Where: D_{eq} = the equivalent diameter; V = volume.

The real specific masses (ρ) and the apparent specific masses (ρ_{ap}) were determined by the picnometry method. With the specific mass determined, Geldart's diagram classification was possible.

In order to determine the samples' specific mass, the pycnometry was performed with water, according to the NP EN 1097-6 (IPQ, 2017). The real specific mass of the sand and the mineral coal used were obtained through this analysis. However, real specific mass of the biomass was not obtained due to the low density of its particles. We used for it the helium gas pycnometry in a micromeritics, model AccuPcy II® 13 pycnometer.

The mass of material necessary to fill a 1 L beaker was weighed to obtain the material's bulk mass density. The apparent specific mass was determined by the ratio obtained between the mass of the material and its apparent volume.

In the present research, we chose the use of the Eucalyptus chips as they are disposed by the industry, without any previous preparation. The coal was previously milled in a Marconi® MA340 knife mill, grinding the material so that it passed through a 7 mesh Tyler's series sieve. The sand used was grinded, so that it passed through a 35 mesh Tyler's series sieve.

For the thermogravimetric analyzes (TGA), the fuels were previously milled in a Marconi® MA340 knife mill, grinding the material so that it passed through a 16 mesh Tyler's series sieve. For the TGA, 20 mg of Eucalyptus and 20 mg of coal was used.

Mixtures' preparation

The mixtures of biomass + sand, and coal + sand were made in different mass proportions, containing 3, 5 and 10% of the combustible material (Eucalyptus chips or coal) supplemented by the addition of the inert material (sand).

Fluidization bench

The fluidization was performed on the pilot plant's bench of the CIENTEC's Department of Process Engineering. It was composed by 1) Air compressor; 2) Gate value; 3) U-Tbe manometer; 4) Air-flow meter; 5) Bed distributor; and 6) Fluidized bed column.

The fluidized bed column is made of transparent acrylic. It was constructed in trapezoid format to maintain the same proportions with the dimensions of the pilot plant fluidized bed reactor.

The bench plant system has a bed air distributor composed of a set of air injectors connected to the tube located at the base of the fluidizer.

The compressor supplied air to the bench system, which through regulation of the drawer valve adjusted the airflow for the material's fluidization. The analysis of the profiles and the comparison of the minimum fluidization velocities were evaluated through the graphs generated with the pressure drop data in the bed (Δp) as a function of the air velocity injected in bed (u_s).

Binary mixture fluidization

The data were collected, twice on each point, as a function of the inflow of air in the bed [m s^{-1}] by the drop of bed pressure [mmH$_2$O]. After the data's treatment (utilizing 1 mmH$_2$O = 9.806159 Pa), graphs were generated for the analysis and the experimental determination of the points corresponding to the apparent (u_{fa}) and the minimum (u_{mf}) fluidization velocities.

In the fluidization process, the produced curves were used to determine the apparent fluidizing velocity, according to Kunii & Levenspiel (1991) method, due to the appearance of the pressure drop's peak, because of the passage from the bed's state from fixed to fluidized. With the defluidization curves, the minimum fluidization velocity was determined, referring to the bed's return point from the fluidized to the fixed state.

Results

The results of the immediate analysis, elemental analysis and the lower calorific value (LCV) are presented in Table 1. A 9.3% for Eucalyptus chips and 22.0% for coal was obtained as C fixed. The volatile matter of Eucalyptus chips was 85.8%, and 23.0% for coal. The percentage of C was higher in the Eucalyptus chips (54.2) than in coal (33.8%). Sulfur and nitrogen were not detected in the Eucalyptus chips sample, and they were very low in the coal samples. Oxygen proportion present in the Eucalyptus chips were much higher than in the coal samples (40.2% and 6.4%, respectively).

The thermogravimetric analysis (TGA) curves for samples of coal, Eucalyptus chips, and a mixture

(70% coal + 30% Eucalyptus chips) are presented in Figure 1. Three distinct regions are presented in the thermal decomposition for both materials and mixture. The first drop of temperature in the thermogravimetric analysis curve is at a rise up of approximately 100 °C. A second mass loss region can be identified from 230 °C to 300 °C. At approximately 440 °C we can observe the occurrence of the third biomass' loss. The coal sample had a little mass' loss up to 300 ºC in the TGA analysis. Between 300 °C and 450 °C we observed a significant loss of mass.

Table 2 summarizes the parameters used to classify the materials according to Geldart´s diagram. We used air as gas to fluidize (density corresponding to 0.00121 g cm⁻³).

Coal and Eucalyptus chips are classified in the "D group" and sand in the "B group" according to the Geldart's classification.

Fluidization and Defluidization

The pressure drop (ΔP) measured as a function of the gas (air) surface velocities for the different concentrations of combustible material inside the sand fluidized bed are demonstrate in Figures 2 to 5. The values for fluidization velocities and pressure drop are presented in Table 3. The variation of the minimum fluidization velocities obtained in the bench scale, as a function of the percentages of the materials used in the sand bed is shown in Figure 6.

Table 1. Immediate analysis, elemental analysis and calorific value of Ecalyptus chips and coal

| | | Combustible material | |
		Eucalyptus chips	Coal
Immediate analysis (% mass)	C fixed [a]	9.3	22.0
	Ashes [a]	0.3	55.0
	Volatile matter [a]	85.8	23.0
	Humidity	4.6	17.1
Elemental analysis (% mass)	C [a]	54.2	33.8
	H [a]	5.7	2.30
	S [a]	nd	1.90
	N [a]	nd	0.60
	O [a]	40.2	6.40
Calorific value (kJ kg⁻¹)	Lower calorific value [b]	19,150	10,112.7

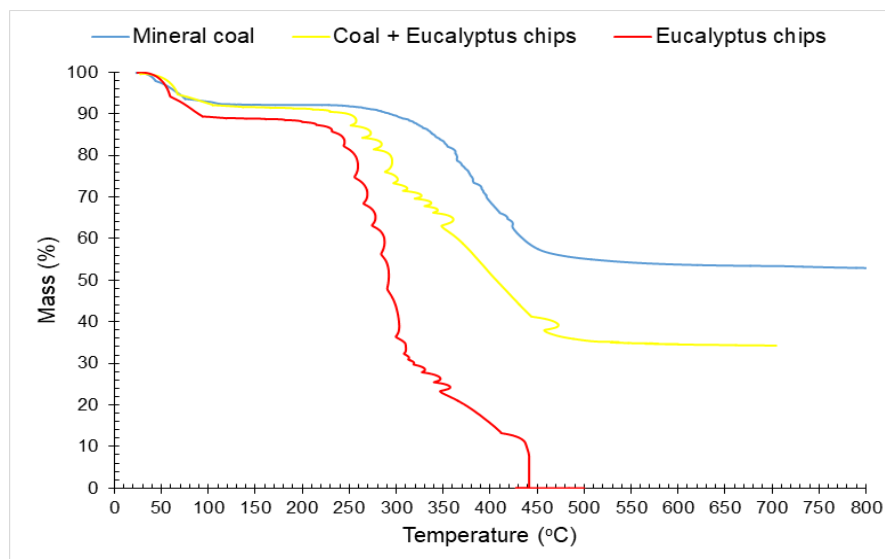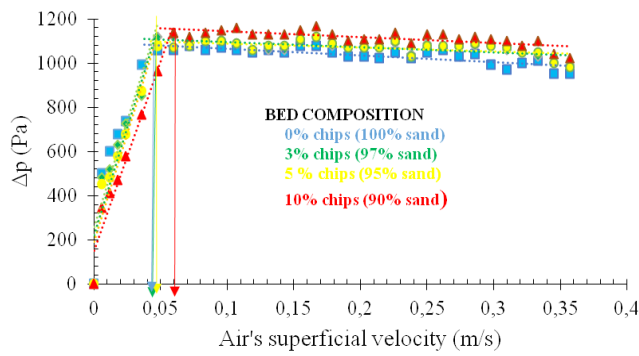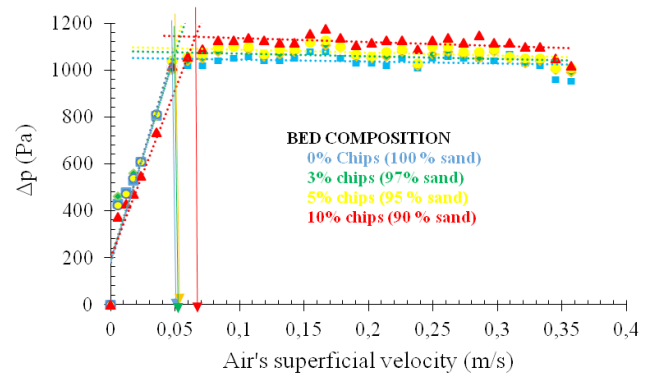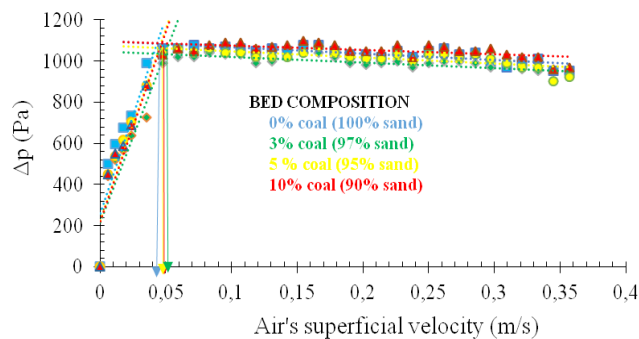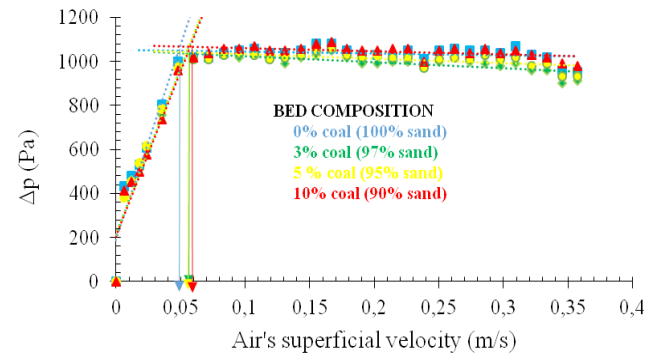a = dry basis; b = wet basis; nd = No detection.

Figure 1. Thermogravimetric analysis (TGA) thermal analysis curves for the used combustible materials' samples.

A. G. Auler1 et al.

Table 2. Geldart's classification of the used materials.

Material	ρ [g cm⁻³]	ρ_ap [g cm⁻³]	ρ-ρ_air [g cm⁻³]	Mean diameter [mm]	Geldart's classification
Coal	1.66	1.37	1.659	0.48	D
Eucalyptus chips	0.530	0.282	0.529	5.03	D
Sand	2.55	2.46	2.549	0.31	B

Figure 2. Fluidization with different percentages of Eucalyptus chips in the bed.

Figure 3. Defluidization with different percentages of eucalyptus chips in the bed.

Figure 4. Fluidization with different percentages of mineral coal in the bed.

Figure 5. Defluidization with different percentages of mineral coal in the bed.

Table 3. Fluid dynamics in sand, coal and in Eucalyptus chips.

Material	Mass (%)	u_fa [m s⁻¹]	Δp (Pa)	u_mf [m s⁻¹]	Δp (Pa)
Sand	100	0.043	1,083. 95	0.05	1,077.54
Coal	3	0.049	1,035.57	0.049	1,030.85
	5	0.045	1,063.33	0.049	1,033.25
	10	0.047	1,085.56	0.052	1,051.54
Eucalyptus chips	3	0.046	1,109.69	0.050	1,077.22
	5	0.049	1,098.67	0.051	1,093.04
	10	0.054	1,153.78	0.066	1,142.13

u_{fa}: Apparent fluidization velocity; u_{mf}: Minimum fluidization velocity; **m s⁻¹**: meter per second; **Δp**: Pressure drop; **Pa**: Pascal.
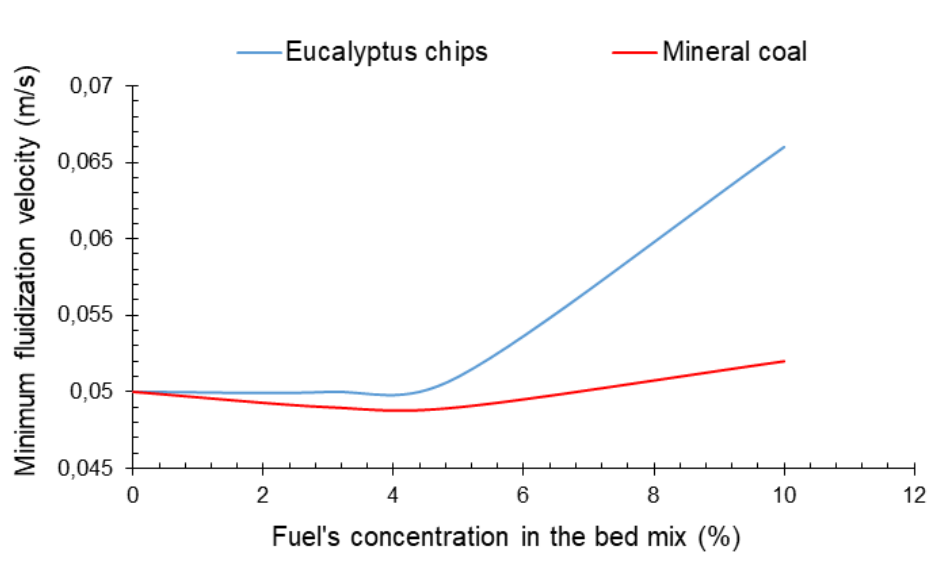
Figure 6. Minimum fluidization velocity (u_{mf}) as a function of the percentage of combustible materials and mixtures.

Discussion

If a material has over 50% (dry basis) of elemental carbon material, it can be harnessed energetically (Abreu, 2015; Basu, 2006). The results of the elemental analysis show C = 54.24% for the Eucalyptus chips suggesting that this material can be an excellent solid fuel.

Ngangyo-Heya et al. (2016) suggest that the chemical composition of a material influence significantly the heating value. Higher moisture and ash content in the material results in lower calorific value.

The analysis of the calorific value of the fuels used in thermochemical processes is fundamental. The calorific value is defined as the amount of energy released in the form of heat during the combustion of a defined quantity (mass) of a material (Van Loo & Koppejan, 2010). When the combustion occurs in a boiler, it will generate heat; the heat will move the turbines and it will produce electricity. As higher the amount of heat generated, higher is the pressure produced in the boiler. Therefore, when the calorific value of the material used in the bed filling is higher, is the power generated in the turbine will be higher (Linhares, 2016).

Three distinct regions are presented in the thermal decomposition for both materials and mixture (Figure 1). There are two well-defined mass losses sections and one discrete mass loss section.

According to Magdziarz & Wilk (2013), the release of moisture content forms the first drop temperature in the thermogravimetric analysis (TGA) curve at a rise up of approximately 100 ºC. The values obtained in the determination of moisture for the Eucalyptus chips (4.62%), and for the mineral coal (8.5%) coincide on the first drop with the values obtained through the TGA.

Following the biomass' temperature increment, as observed in Figure 1, a second mass loss region can be identified from 230 °C to 300 °C. This mass loss is related to the decomposition of cellulose and hemicellulose present in the biomass (Magdziarz & Wilk, 2013). The degradation of hemicelluloses occurs between 230-290 °C, and the cellulose degrades between 275-500 ºC (Seye et al. 2013; Pereira et al., 2013; Granados et al., 2017).

At approximately 440 °C we can observe the occurrence of the third biomass' loss, which is related to the lignin's degradation (Pécora et al., 2014). According to Pereira (2017), below 500 °C about 40% of the lignin decomposes, while the remainder is degraded at higher temperatures.

The coal sample submitted had a little mass' loss up to 300 ºC in the TGA analysis. Between 300 °C and 450 °C we observed a significant loss of mass due to the degradation of the carboxyl groups present in the coal (Silva et al., 2018). A high amount of ash was remaining after the temperature exceeded 450 °C. The amount of ash obtained at the end of the TGA of the Eucalyptus chips was near to null, resembling the quantities of ash found through the immediate analysis (0.30%). Similarly, the value higher than 50% for the

A. G. Auler1 et al.

mineral coal's TGA was also obtained, with ash content being 55%. The ash is responsible for the coal's mass percentage constancy, even at higher temperatures (Bada et al., 2015).

According to Linhares (2016), the density differences between combustible materials and the heterogeneity can result in segregation problems within a reactor and it may cause a difference in the bed temperature on co-combustion processes.

In Table 2, it can be observed that the chips' and coal's classification, referring to Geldart's classification, belongs to the group D. This group is characterized by composing a high-density and larger particulate size, requiring a high gas flow for the fluidization process. The bubbles that are formed during the process tend to rise slowly due to a larger component of the particulates' weight. The particles of this type of fluidization are larger than 1000 μm (Shaul et al., 2014).

It was observed a similar pattern regarding the pressure drop curves (Figures 2 to 5). The total pressure drop (ΔP) increased with increasing gas velocity, and the particles remained stagnant (characterizing fixed bed). As the surface velocity increased, the accessible force caused by the pressure drop became similar to the apparent weight of the bed solids and, following the air velocity's increase, the bed was fully fluidized.

The graphical methods presented by Kunii & Levenspiel (1991) and Chiba (1979) were applied in the graphs of Figures 2 to 5 to determine the apparent fluidization (u_{af}) and minimum fluidization velocities (u_{mf}), respectively.

The fluidization curves of mixtures containing Eucalyptus chips (Figures 2 and 3) were performed in different chips' mass proportions, in order of 3, 5, and 10%, with no formation of preferential paths being observed in these proportions. Gomes (2017), using Eucalyptus chips with diameters smaller than 4 mm concluded that the fluidization would occur until 28% mass fraction.

Among the coal + sand mixtures (Figures 4 and 5) in combustible mass proportions 3, 5 and 10%, small differences were observed in the u_{af}, u_{mf} and pressure drop when compared with the bed formed exclusively by sand.

When the proportion of combustible material was added, the u_{mf} increased (Figure 6), being emphasized the introduction of Eucalyptus chips in the bed's composition. By the utilization of coal and sand only,

the u_{mf} did not vary significantly with the increase of coal concentration in the bed. Particles become fluidized when an upward-flowing gas imposes a high enough drag force to overcome the downward force of gravity. This effect is minimal for spherical particles like the coal ones, but the influence of the drag force is more significant for irregularly shaped particles, like the Eucalyptus chips ones (Cocco et al., 2014).

The preferred paths emergence can be observed by the increment of the fluid's pressure drop (ΔP). This increase in the velocity is necessary for the fluidization occurrence, with the biomass addition to the sand. The pressure drop (ΔP) decreased with increasing biomass concentration in the bed (Gomes et. al, 2017).

This reduction can occur because of the specific mass difference. The drag force necessary to fluidize the particle is smaller than the weight force. For fluidization to occur, the drag force exerted by the bed must be equal to the force weight in the particle besides the shape and the average (Cocco et al., 2014) diameter of the particle. About the shape, spherical particles do not change in the component of the drag force as their position varies. In non-spherical particles, the position of the particle diverges the value of the modulus of the drag force ; thus, in particles with a flat shape, they have diverse values of the drag force (Dioguardi; Mele, 2015) according to the position in which they are.

Another way of understanding this reduction is the formation of preferential paths. When the air passes through preferred paths, it suffers little or no opposition from the bed's particles, which causes a small or zero pressure drop (Geldart, 1986). In this case, increasing the airflow velocity is necessary to undo the preferred paths. Thus, the minimum fluidization velocity increment is observed. In contrast, this addition is responsible for causing the entrainment of particles with lower specific mass, out of bed, causing an undesirable effect of bed loss (Linhares, 2017).

Conclusion

Fluidization of Eucalyptus chips with mineral coal may be possible for application in the combustion process in a pilot plant of bubbling fluidized bed. The results can motivate future theoretical and experimental studies involving the application of this methodology in the development of cleaner and sustainable technologies.

Acknowledgments

References

ABNT. Associação Brasileira de Normas Técnicas. **NBR 8289 (MB 1891)**: carvão mineral: determinação do teor de cinzas. Rio de Janeiro, 1983a.

ABNT. Associação Brasileira de Normas Técnicas. **NBR 8290 (MB 1892)**: carvão mineral: determinação do teor de matérias voláteis. Rio de Janeiro, 1983b.

ABNT. Associação Brasileira de Normas Técnicas. **NBR 8293 (MB 1893)**: carvão mineral: determinação de umidade. Rio de Janeiro, 1983c.

ABNT. Associação Brasileira de Normas Técnicas. **NBR 8299 (MB 1899)**: carvão mineral: determinação do carbono fixo. Rio de Janeiro, 1983d.

ABNT. Associação Brasileira de Normas Técnicas. **NBR 8628 (MB 2063)**: carvão mineral: determinação do poder calorífico superior e do poder calorífico inferior. Rio de Janeiro, 1984.

Abreu, S. M. C. Avaliação de tecnologias de leitos fluidizados a partir da análise dos pedidos de patentes. **Cadernos de Prospecção**, v. 8, n. 3, p.522-529, 2015. http://dx.doi.org/10.9771/s.cprosp.2015.008.058.

AGEFLOR. Associação Gaúcha de Empresas Florestais. **A indústria de base florestal no Rio Grande do Sul**: ano base 2015. Curitiba: Consufor, 2016. 96 p. Available from: <http://www.ageflor.com.br/noticias/wp-content/uploads/2016/09/AGEFLOR-DADOS-E-FATOS-2016.pdf>. Access on: 30 Aug. 2017.

AGEFLOR. Associação Gaúcha de Empresas Florestais. **A indústria de base florestal no Rio Grande do Sul**: ano base 2016. Curitiba: Consufor, 2017. Available from: <http://www.ageflor.com.br/noticias/wp-content/uploads/2017/08/A-INDUSTRIA-DE-BASE-FLORESTAL-NO-RS-2017.pdf>. Access on: 05 Sept. 2017.

Anuário mineral brasileiro. Brasília, DF: Departamento Nacional de Produção Mineral, v. 35, 2010. Available from: < http://www.anm.gov.br/dnpm/paginas/anuario-mineral/arquivos/anuario-mineral-brasileiro-2010>. Access on: 2 Sept. 2017.

Bada, S. O. et al. Characterization and co-firing potential of a high ash coal with Bambusa balcooa. **Fuel**, v. 151, p. 130-138, 2015. http://dx.doi.org/10.1016/j.fuel.2015.01.068.

Basu, P. **Combustion and gasification in fluidized beds**. [S.l.]: Crc Press, 2006. 496 p.

Basu, P. & Zhi-Gang, P. Prediction of minimum fluidization velocity for binary mixtures of biomass and inert particles. **Powder Technology**, v. 237, p. 134-140, 2013. http://dx.doi.org/10.1016/j.powtec.2013.01.031.

Bioetanol de cana-de-açúcar: energia para o desenvolvimento sustentável. Rio de Janeiro:BNDES, 2008. 316 p. Disponível em: <https://web.bndes.gov.br/bib/jspui/handle/1408/2002>. Access on: 14 Agu 2019.

Brasil. Ministério de Minas e Energia. CGTE Eletrobras. **Candiota**. Available from: <http://cgtee.gov.br/UNIDADES/CANDIOTA>. Access on: 13 Aug. 2019.

Brasil. Ministério de Minas e Energia. Carvão Mineral. **Portal Brasil**. [2011]. Available from: <http://www.brasil.gov.br/infraestrutura/2011/11/carvao-mineral>. Access on: 3 Sept. 2017.

Chiba, S. et al. The minimum fluidization velocity, bed expansion and pressure-drop profile of binary particle mixtures. **Powder Technology**, v. 22, n. 2, p. 255-269, 1979. http://dx.doi.org/10.1016/0032-5910(79)80031-5.

Cocco, R. et al. **Introduction to fluidization**. Chemical Engineering Progress, p. 21-29, 2014. Available from: <https://www.aiche.org/sites/default/files/cep/20141121.pdf>. Access on: 14 Agu. 2019.

Dioguardi, F. & Mele, D. A new shape dependent drag correlation formula for non-spherical rough particles. Experiments and results. **Powder Technology**, v. 277, p. 222-230, 2015. http://dx.doi.org/10.1016/j.powtec.2015.02.062.

Eichler, P. et al. Produção do biometanol via gaseificação de biomassa lignocelulósica. **Química Nova**, v. 38, n. 6, p. 828-835, 2015. http://dx.doi.org/10.5935/0100-4042.20150088.

Geldart, D. Types of gas fluidization. **Powder Technology**, v. 7, p. 285-292, 1973. https://doi.org/10.1016/0032-5910(73)80037-3.

Geldart, D. **Gas fluidization technology**. New York: John Wiley & Sons, 1986.

Gomes, L. et al. Preliminary study of fluidization curves in polydisperse beds formed by a binary mixture of *Raphanus sativus* L. Husk and Sand. Oalib. **Scientific Research Publishing**, v. 4, n. 8, p. 1-10, 2017. http://dx.doi.org/10.4236/oalib.1103713.

Granados, D. A et al. Study of reactivity reduction in sugarcane bagasse as consequence of a torrefaction process. **Energy**, v. 139, p. 818-827, 2017. http://dx.doi.org/10.1016/j.energy.2017.08.013.

IEA. International Energy Agency. **World Energy Outlook 2016**. Paris, 2016. 684 p. https://doi.org/10.1787/weo-2016-en.

IBÁ. Indústria Brasileira de Árvores. **Relatório 2017**. Brasília, DF, 2017. 80 p. Available from: <https://iba.org/images/shared/Biblioteca/IBA_RelatorioAnual2017.pdf>. Access on: 14 Agu. 2019.

Instituto Português de Qualidade. **NP EN 1097-6**: ensaios das propriedades mecânicas e físicas dos agregados: parte 6: determinação da massa volúmica e da absorção de água. Caparica, 2016. Available from: <https://lojanormas.ipq.pt/product/np-en-1097-6-2016/>. Access on: 05 Sept. 2017.

Kunii, D. & Levenspiel, O. **Fluidization engineering**. 2. ed. Saint Louis: Elsevier, 1991. 491 p.

Linhares, F. de A. de et al. Avaliação fluidodinâmica e co-combustão de resíduo de biomassa industrial em planta de bancada e planta piloto de leito fluidizado borbulhante In: FORUM INTERNACIONAL DE RESIDUOS SOLIDOS, 7., 2016, Porto Alegre. **Anais**. Porto Alegre: Instituto Venturi Para Estudos Ambientais, 2016. p. 1 - 10. Avaliable from: <http://www.firs.institutoventuri.org.br/images/T006_AVALIAÇÃO_FLUIDODINÂMICA_E_COCOMBUSTÃO_DE_RESÍDUO_DE_BIOMASSA_INDUSTRIAL_EM_PLANTA_DE_BANCADA_E_PLANTA_PILOTO_DE_LEITO_FLUIDIZADO_BORBULHANTE.pdf>. Access on: 12 Sept. 2017.

Magdziarz, A. & Wilk, M. Thermal characteristics of the combustion process of biomass and sewage sludge. **Journal of Thermal Analysis and Calorimetry**, v. 114, n. 2, p. 519–529, 2013. https://doi.org/10.1007/s10973-012-2933-y.

Ngangyo-Heya, M. et al. Calorific value and chemical composition of five semi-arid mexican tree species. **Forests**, v. 7, n. 12, p. 58-70, 4 2016. http://dx.doi.org/10.3390/f7030058.

Patterson, R. K. Automated Pregl-Dumas technique for determining total carbon, hydrogen, and nitrogen in atmospheric aerosols. **Analytical Chemistry**, v. 45, n. 3, p.605-609, 1973. http://dx.doi.org/10.1021/ac60325a050.

Paudel, B. & Feng, Z. Prediction of minimum fluidization velocity for binary mixtures of biomass and inert particles. **Powder Technology**, v. 237, p. 134-140, 2013. http://dx.doi.org/10.1016/j.powtec.2013.01.031.

Pécora, A. A. B. et al. Prediction of the combustion process in fluidized bed based on physical-chemical properties of biomass particles and their hydrodynamic behaviors. **Fuel Processing Technology**, v. 124, p. 188–197, 2014. https://doi.org/10.1016/j.fuproc.2014.03.003.

Pereira, B. L. C. et al. Estudo da degradação térmica da madeira de *Eucalyptus* através de termogravimetria e calorimetria. **Revista Árvore**, v. 37, n. 3, p. 567-576, 2013. http://dx.doi.org/10.1590/s0100-67622013000300020.

Pereira, J. L. **Análise da qualidade do gás de síntese produzido em gaseificadores de leito fixo co-corrente para potencial aplicação em microturbinas a gás**. 2017. 65 f. Dissertação (Mestrado em Engenharia de Energia) – Universidade Federal de Itajubá, Itajubá.

Phitsuwan, P. et al. Improvement of lignocellulosic biomass in planta: A review of feedstocks, biomass recalcitrance, and strategic manipulation of ideal plants designed for ethanol production and processability. **Biomass and Bioenergy**. v. 58, p. 390-405, 2013. https://doi.org/10.1016/j.biombioe.2013.08.027.

Rambo, M. K. D. et al. Analysis of the lignocellulosic components of biomass residues for biorefinery opportunities. **Talanta**. v. 144, p. 696–703, 2015. https://doi.org/10.1016/j.talanta.2015.06.045.

Santos, F. et al. **Bioenergia e biorrefinaria**: cana-de-açúcar e espécies florestais. Viçosa, MG: Ed. UFV, 2013.

Seye, F. et al. Effect of humic and application at different growth stages of kinnow mandarin (citrus reticulata blanco) on the basis of physio-biochemical and reproductive responses. **Academia Journal of Biotechnology**, v. 1, n. 1, p. 046-052, 2013.

Shaul, S. et al. Typical fluidization characteristics for geldart's classification groups. **Particulate Science And Technology**, v. 32, n. 2, p. 197-205, 2014. http://dx.doi.org/10.1080/02726351.2013.842624.

Silva, V. S. et al. Caracterização de resíduos gerados na colheita e no beneficiamento da macieira para fins energéticos em leitos fluidizados polidispersos. **Estudos Tecnológicos em Engenharia**, v. 12, n. 2, p. 45-67, 2018. http://dx.doi.org/10.4013/ete.2018.122.03.

Smolinski, A. et al. A comparative experimental study of biomass, lignite and hard coal steam gasification. **Renewable Energy**, v. 36, n. 6, p. 1836–1842, 2011. https://doi.org/10.1016/j.renene.2010.12.004.

Suksankisorn, K. et al. Co-firing of Thai lignite and municipal solid waste (MSW) in a fluidized bed: effect of MSW moisture content. **Applied Thermal Engineering**, v. 30, n. 17-18, p. 2693–2697, 2010. https://doi.org/10.1016/j.applthermaleng.2010.07.020.

UNFCCC. United Nations Climate Change. **Annex 8**: clarifications on definition of biomass and consideration of changes in carbon pools due to a CDM project activity. (UNFCCC/CCNUCC. EB 20 Report, Annex 8, p. 1). Available from: <https://cdm.unfccc.int/Reference/Guidclarif/mclbiocarbon.pdf>. Access on: 14 Agu 2019.

Van Loo, S. &; Koppejan, J. **The Handbook of biomass combustion and co-firing**. London: Earthscan Publications, 2010. 442 p.

Vaz Junior, Sílvio et al (Ed.). **Biorrefinarias**: cenários e perspectivas. Brasília, DF: Embrapa Agroenergia, 2011. 175 p.

Vaz Júnior, S. & Soares, I. P. Chemical analysis of biomass-a review of techniques and applications. **Química Nova**, v. 37, n. 4, p. 709-715, 2014. https://dx.doi.org/10.5935/0100-4042.20140111.